The dynamics and heating of the quiet solar chromosphere

Wolfgang Kalkofen*,† and Peter Ulmschneider**

*Harvard-Smithsonian Center for Astrophysics, 60 Garden St., Cambridge, MA02138, USA
**Institut für Theoretische Astrophysik, Universität Heidelberg, Tiergartenstr. 15, Germany

The solar chromosphere can be characterized by two signatures: the spectroscopic signature is an emission spectrum for all radiation originating in the chromosphere; only NLTE effects in the cores of strong lines producing absorption features. And the dynamical signature is in the form of oscillations, with a period of 3 min in the nonmagnetic chromosphere and a period of 7 min in magnetic regions.

The paper explains these signatures in terms of waves: The dynamics of the chromosphere is due to acoustic waves in the magnetic-field-free atmosphere, which produce K_{2v} bright points, and to kink and longitudinal waves in magnetic flux tubes, which produce network bright points. The heating of the chromosphere is caused by acoustic waves whose dissipation makes the kinetic temperature rise in the outward direction, producing the emission spectrum. As far as energy fluxes are concerned, the energy dissipated in chromospheric heating outweighs the energy visible in bright points by two orders of magnitude.

The paper interprets the observed oscillation periods in the chromosphere as cutoff periods: for the 3 min period, as the cutoff period of acoustic waves in a nonmagnetic, stratified atmosphere; and for the 7-min period, as the cutoff period of kink waves in magnetic flux tubes for field strengths typical of the magnetic network.

1. Introduction

THE most prominent lines in the visible spectrum of the chromosphere are the H and K lines of Ca II. Their emission shows a separation of the atmosphere into nonmagnetic and magnetic regions, which are referred to as internetwork and magnetic network or, because of their connection to convection, as interior and boundary of supergranulation cells. This bifurcation of the medium is further emphasized by the dynamical behaviour, which shows oscillations with periods of 3 min in the internetwork chromosphere and 7 min in the network[1] (Figure 1). Furthermore, the time variation of the intensity is different: The 3-min oscillations are marked by a sharply-peaked time variation of the intensity[2] and a strong preference for the blue emission peaks, H_{2v} and K_{2v}, and the 7-min oscillations are accompanied by a broad time variation of the intensity and a much less pronounced preference for the blue peaks[3]. The bifurcation of the chromosphere that characterizes optical lines is also found in the ultraviolet, where SUMER shows 3-min waves in emission lines and continua of neutral metals from the internetwork chromosphere[4], and 7-min waves in emission of the Lyman continuum and several Lyman lines from the magnetic network[5].

In contrast to the dynamics, the differences in the appearance of emission lines and continua are minor, especially those from the layers of the low chromosphere[6]. It is therefore likely that the nonmagnetic and magnetic chromospheres are heated by the same mechanism. It is also noteworthy that the chromosphere produces emission everywhere and all the time[4] and never the absorption spectrum predicted by the chromospheric bright point model of Carlsson and Stein[7,8].

The observations of chromospheric radiation thus suggest a separation of the description of chromospheric phenomena into (1) the dynamics of K_{2v} bright points with 3-min oscillations of large amplitude at a few, select points in the internetwork medium, and the dynamics of network bright points with 7-min oscillations of large amplitude in magnetic flux tubes and (2) the general heating of the chromosphere. The paper is structured

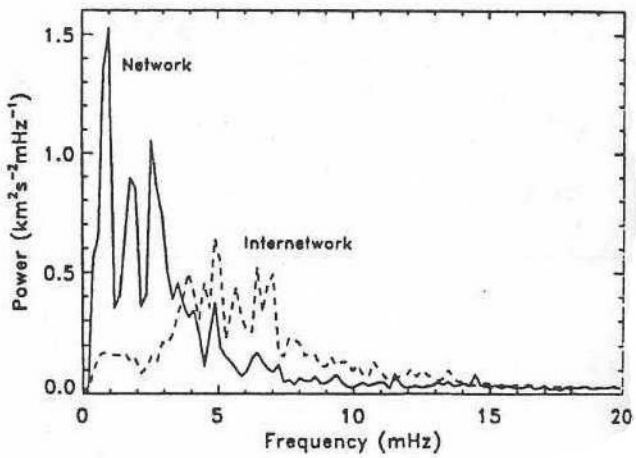

Figure 1. Velocity power spectra from the Doppler motion of the H_3 absorption minimum of the H line, at disk center. Network and internetwork regions along the slit are averaged separately. From Lites *et al.*[1].

†For correspondence. (e-mail: wolf@cfa.harvard.edu)

accordingly: Section 2 discusses chromospheric dynamics on the basis of the hydrodynamic and magnetohydrodynamic equations. Section 3 considers the general chromospheric heating requirements, while in Section 4 the generation of acoustic waves in the convection zone and the dissipation of this energy by weak acoustic shocks is outlined. Section 5 summarizes the paper.

2. Chromospheric dynamics

Waves in the chromosphere are affected by the density stratification due to gravity, which makes waves dispersive, and introduces cutoffs that separate propagating from evanescent frequencies. For acoustic waves in the nonmagnetic medium, where gas pressure provides the restoring force in the wave equation, the cutoff frequency, ν_{ac}, at the temperature minimum between photosphere and chromosphere is equal to 5 mHz (cutoff period $P_{ac} = 1/\nu_{ac} = 3$ min). Waves with frequencies lower than ν_{ac} are evanescent, i.e. their phase velocity is infinite and their group velocity is zero; thus they transport no energy (in the low-amplitude limit). For internal-gravity waves in the nonmagnetic medium, where gravity provides the restoring force in the wave equation, the cutoff frequency is the Brunt-Väisälä frequency, N_{BV}. Waves with frequencies lower than N_{BV} can propagate, but they are excluded from the purely vertical direction. In a neutral, monatomic gas, N_{BV} and ν_{ac} have practically the same value. Thus the two cutoff frequencies separate the wave spectrum into the regimes of low frequencies, where only internal-gravity waves can propagate, and high frequencies, where only acoustic waves can.

In the magnetic chromosphere, two wave-modes play a role, namely, longitudinal flux tube waves, where gas pressure provides the main restoring force, and transverse flux tube waves, or kink waves, where the magnetic field does[9]. For the magnetic-field strengths encountered in the quiet network, the cutoff frequencies are $\nu_\lambda = 5$ mHz ($P_\lambda = 3$ min) for the longitudinal mode, and $\nu_\kappa = 2.5$ mHz ($P_\kappa = 7$ min) for the kink mode. For both wave-modes, propagating waves have frequencies above the cutoff, and evanescent waves, below the cutoff.

A dynamical model by Carlsson and Stein[7] of the nonmagnetic chromosphere combined a sophisticated hydrodynamic code, incorporating NLTE radiative transfer of the Ca II ion, with empirical driving, which was taken from the Doppler velocity measured in a photospheric Fe-I line in an hour-long observing run[1]. The empirical approach sacrificed the search for the underlying cause of the oscillations, but, in return, allowed firm conclusions about the nature of the K_{2v} phenomenon. Since the simulation[7] reproduced to high fidelity the intricate intensity and velocity variations in the core of the H line for two out of the four bright points from the same observing run, it is clear that the waves powering K_{2v}-bright points are propagating acoustic waves.

In the network bright points on the supergranulation cell boundary, the periods of oscillation, typically near 7 min, are longward of the acoustic cutoff period and of the Brunt-Väisälä period, where acoustic waves are evanescent but internal-gravity waves propagate. Some observers have therefore considered the waves in the magnetic network to be internal-gravity waves[10,11]. A theoretical underpinning of this hypothesis by Lou[12] found the observed periods to be possible as resonances of magneto-gravity waves in a chromospheric cavity. But a heuristic picture of network bright points in terms of internal-gravity waves by Deubner and Fleck[13] was shown by Kalkofen[14] to fail in its intended purpose, namely, to dissipate the wave energy in traveling downward in the narrowing flux-tube funnels.

An explanation of network bright points not based on oscillations in a cavity was proposed by Kalkofen[14] who noted the coincidence of the observed oscillation period with the cutoff period of kink waves for magnetic field strengths found in the magnetic network. Numerical modeling by Choudhuri *et al.*[15] and the analytic solution of the MHD equations for impulsive excitation[16] showed that oscillations at the cutoff could indeed be produced. In order to dissipate, however, the transverse waves have to transfer energy to the longitudinal mode, which forms shocks[17].

Wave excitation in a magnetic flux tube produces both transverse and longitudinal waves. But the power spectrum of waves in the network shows virtually no power at 5 mHz, the cutoff frequency of the longitudinal mode. The scenario for network-bright points therefore requires the wave excitation to produce mainly transverse waves. This is indeed the case, as was shown with numerical solutions[18] and with analytic methods[19].

A consequence of the almost exclusive excitation of transverse waves is that a significant flux in longitudinal waves appears only in the chromosphere, where the nonlinearity of the waves facilitates the transfer of energy between modes. This transfer is consistent with the low value of the observed velocity coherence between the base and the middle of the network chromosphere[1] (Figure 7), which indicates that the dissipating longitudinal waves do not arrive from below but are formed in the chromosphere.

For the analytic modeling of chromospheric oscillations we consider the hydrodynamic equations. From a small-amplitude expansion of the equations for a one-dimensional, isothermal atmosphere we obtain the Klein–Gordon equation[20]:

$$\frac{\partial^2}{\partial z^2}u - \frac{\partial^2}{\partial t^2}u - u = 0, \qquad (1)$$

which is written here for the 'reduced' velocity u and in terms of the dimensionless depth and time variables z

and t. For acoustic waves, the 'physical' velocity v is obtained as

$$v(\zeta, \tau) = \mu(\zeta, \tau)e^{\zeta/2H}, \quad (2)$$

in terms of the physical depth and time variables ζ and τ.

The derivation of the wave equation (1) for acoustic waves assumes that the atmosphere is one-dimensional, isothermal and stratified in plane-parallel layers with a constant scale height H. In the vertical direction, only acoustic waves are allowed (i.e. internal-gravity waves are excluded from the vertical direction). The velocity v grows exponentially with height ζ with a scale length of twice the density-scale height.

Magnetic waves propagating in the expanding geometry of a thin magnetic flux tube, in pressure equilibrium with the surrounding medium, satisfy the same wave equation[20], but with different definitions of the dimensionless variables. An additional requirement (which is satisfied here) is a constant ratio $\beta(= 8\pi p/B^2)$ of gas to magnetic pressure inside the tube. The physical velocity v is now obtained as

$$v(\zeta, \tau) = u(\zeta, \tau)e^{\zeta/4H}, \quad (3)$$

showing slower exponential growth for tube modes, with a scale length of $4H$ because of exponential spreading of the tube cross section.

The solution of the wave equation for a velocity impulse at $z = 0$ and $t = 0$, in an infinite medium is given by Lamb[21],

$$u(z, t) = \tfrac{1}{2}\delta(t - |z|) - \frac{t}{2}\frac{J_1(\sqrt{t^2 - z^2})}{\sqrt{t^2 - z^2}}\mathcal{H}(t - |z|), \quad (4)$$

where δ is the Dirac δ-function; $\mathcal{H}$ is the Heaviside function and J_1 is a Bessel function. The argument of both the δ-function and the Heaviside function expresses the propagation of the head of the wave ($|z| = t$), at the sound speed for acoustic waves and at the tube speeds for the flux-tube waves. The tube speeds in dimensioned units are given by $c_\lambda = c_s[2/(2 + \gamma\beta)]^{1/2}$ for the longitudinal mode, and $c_\kappa = c_s[2/(\gamma(1 + 2\beta))]^{1/2}$ for the transverse mode, where c_s is the sound speed and $\gamma(= 5/3)$ is the ratio of specific heats.

Behind the head of the wave, the atmosphere oscillates initially with frequencies in a broad spectrum, but this narrows with time until it results in an oscillation at the cutoff[22], as shown by the asymptotic solution of the Klein–Gordon equation:

$$u(z, t) \sim \frac{\cos(t)}{\sqrt{t}}, \quad t \gg z \geq 0, \quad (5)$$

in which the (reduced) velocity becomes independent of height z. The solution implies that gas elements at all heights reach maximal amplitude simultaneously. At the cutoff[22] frequency, the phase velocity, which is given by

$$v_\phi = \frac{\omega}{\sqrt{\omega^2 - 1}}, \quad v_{\text{group}} = 1/v_\phi, \quad (6)$$

is infinite and the group velocity is zero.

In dimensioned units, the cutoff periods are given by

$$P_{ac} = 4\pi H/c_s,$$
$$P_\lambda = P_{ac}\sqrt{(60 + 50\beta)/(63 + 48\beta)}, \quad (7)$$
$$P_\kappa = P_{ac}\sqrt{2\gamma(1 + 2\beta)},$$

for acoustic waves and for longitudinal and transverse flux-tube waves, respectively[22].

It is interesting to note that the highest phase velocities are reached near the origin of the wave, and that they increase with the order of the maximum behind the head of the wave[16]. For comparison with observations it needs to be remembered that these analytic results are for an isothermal atmosphere initially at rest; even the observed values of the photospheric velocity allowed to reproduce the H-line observations only when the waves were launched into a disturbed atmosphere[7].

The asymptotic solution of the Klein–Gordon equation shows that an impulse can excite oscillations at the cutoff of the respective mode. Any sudden change in the forcing function has the same consequence. An example of the former is found in the seismic events following the collapse of an intergranular lane[23], an example of the latter in stochastic excitation[24]. Thus there are two possible models for the generation of K_{2v}-bright points: (1) Individual events at a few, discrete points in the internetwork medium. They might account for the strong bright points observed by Liu (1974)[25] or by Brandt *et al.* (1992)[26] with a filling factor of about 1%, or modeled[7]. (2) Ubiquitous generation of oscillations from the turbulence in the convection zone[27], leading to bright points that are visible anywhere in the K line[2], or in UV lines[4] where they are observed in half the positions along the slit of the SUMER instrument.

For network bright points Muller *et al.*[26] have observed the interaction of fast granules with magnetic-flux tubes. This process was modeled by Choudhuri *et al.*[15], as footpoint motion of a flux tube, resulting in a kink wave in the tube.

While the various processes make plausible the excitation of oscillations at the cutoff of a mode, observational confirmation of a link between a photospheric event and, after a delay accounting for the wave travel time, of a chromospheric brightening is still lacking.

An interesting puzzle is posed by the dynamical modeling of H_{2v}-bright points[7]. On one hand, the simulation reproduced to high accuracy the complex variation of the intensity and shape of the H line, including the

proper time delay between the motion of the photospheric Fe-I line and that of the resulting H line, and on the other hand, it predicted an absorption spectrum from any location in the internetwork chromosphere and most of the time, whereas the observations[4] with SUMER show only an emission spectrum. The high spatial and temporal resolution of the space observations exclude the possibility of spatial and temporal averaging to hide a chromospheric absorption spectrum behind the observed emission. Thus the chromosphere must have a permanent temperature rise in the outward direction, as shown by empirical models. The flaw in the model[7] was traced to the input velocity spectrum by Kalkofen *et al.*[28] who argue that the dynamical model uses only about 1% of the acoustic energy flux available. The hidden flux has frequencies in excess of 10 mHz. The flux critical for the bright point phenomenon is emitted between 5 mHz and 10 mHz. That flux is found in the observed velocity spectrum and accounts for the success of the dynamical simulation. In the following section we address the generation of the flux that is missing from the simulation[7] and treat its dissipation by means of the theory of weak shock waves.

Chromospheric energy losses and the heating requirements

The empirical chromosphere model of Vernazza *et al.*[6] has been constructed by fitting the observed ultraviolet C I, Si I and H I continua with the simulated emission from a hydrostatic equilibrium model with an arbitrary temperature distribution. This temperature distribution was subsequently modified until an optimal fit between the observed and simulated emission was obtained. For the average sun model C, these authors subsequently computed the chromospheric energy-loss rate in H, H^-, Ca II and Mg II due to lines and continua. They found a total radiative energy loss of $F_R = 4.6 \times 10^6$ erg cm^{-2} s^{-1}. Anderson and Athay[29] later improved on this determination by including the abundant line emission from Fe II and found a total chromospheric radiative energy loss of $F_R = 1.4 \times 10^7$ erg cm^{-2} s^{-1}. In addition, they found (see Figure 2) that the cooling rate Φ_R in most of the chromosphere is proportional to the mass density ρ_0, which leads to a characteristic height dependence of the chromospheric emission.

The question is how this persistent energy loss is balanced and how the continuous supply of energy is provided. The time scale in which an excess temperature would cool down to the boundary temperature if the mechanical heating were suddenly disrupted is given by the *radiative relaxation time* for which one has

$$t_{\mathrm{Rad}} = \frac{\Delta E}{\Phi_R} = \frac{\rho c_v \Delta T}{16\bar{\kappa}\sigma T^3 \Delta T} = \frac{\rho c_v}{16\bar{\kappa}\sigma T^3} \approx 1.1\times 10^3 \text{ s}. \qquad (8)$$

Here we used from the VAL81 model that at $z = 1280$ km, $T = 6200$ K, $\rho = 9.8$ dyn/cm^2, $\bar{\kappa}/\rho = 4.1 \times 10^{-4}$ cm^2/g, $c_v = 9.6 \times 10^{-12}$ g/cm^3, $\sigma = 5.6 \times 10^{-5}$ erg/cm^2 s K^4. It is seen that in timescales of a fraction of an hour, the chromosphere would cool down to the boundary temperature if mechanical heating would suddenly stop.

In a purely hydrodynamic environment there are few possibilities to persistently heat a medium: acoustic waves or pulsational waves. For a review on heating mechanisms see Narain and Ulmschneider[30]. Acoustic waves generated in the convection zone are the most likely possibility. To see what acoustic wave heating might do, consider a typical acoustic disturbance in the solar chromosphere. Assume a characteristic perturbation of size $L = 200$ km, temperature $\Delta T = 1000$ K and velocity $\Delta v = 3$ km/s. Using appropriate values for the thermal conductivity $\kappa_{\mathrm{th}} = 10^5$ erg/cm s K and viscosity $\eta_{\mathrm{vis}} = 5 \times 10^{-4}$ dyn s/cm^2 we find for the thermal conductive and viscous heating rates

$$\Phi_C = \frac{d}{dz}\kappa_{\mathrm{th}}\frac{dT}{dz} \approx \frac{\kappa_{\mathrm{th}}\Delta T}{L^2} \approx 3\times 10^{-7}\left[\frac{\mathrm{erg}}{\mathrm{cm}^3\,\mathrm{s}}\right], \qquad (9)$$

$$\Phi_V = \eta_{\mathrm{vis}}\left(\frac{dv}{dz}\right)^2 \approx \frac{\eta_{\mathrm{vis}}\Delta v^2}{L^2} \approx 1\times 10^{-7}\left[\frac{\mathrm{erg}}{\mathrm{cm}^3\,\mathrm{s}}\right]. \qquad (10)$$

These heating are inadequate by a large margin to balance the typical empirical chromospheric cooling rate of 10^{-1} erg/cm^3 s found in the model[6]. Only when the length scale L is decreased by several orders of magnitude can the heating rates be raised to acceptable levels. For acoustic waves, this is accomplished by shock formation. This shows that in pure hydrodynamic situations only

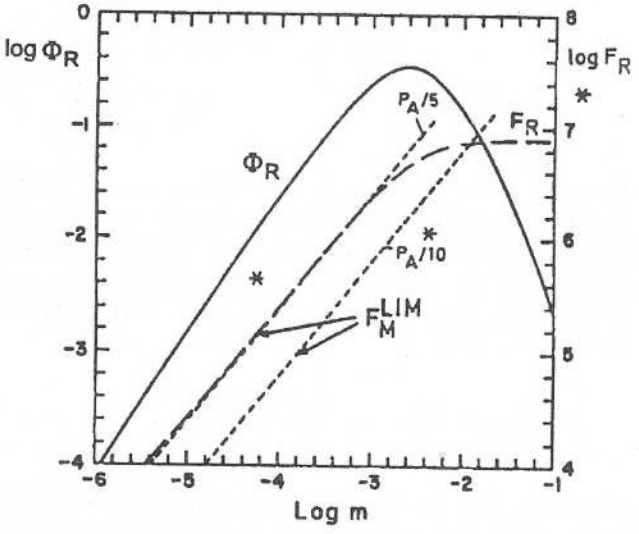

Figure 2. Comparison of the theoretical limiting acoustic flux F_M^{lim} (erg cm^{-2} s^{-1}) with the solar chromospheric radiative loss flux F_r determined empirically by Anderson and Athay[29]. Φ_R (erg cm^{-3} s^{-1}) is the empirical net radiative cooling rate. $P_A/5$ and $P_A/10$ label different assumptions as to the acoustic frequency spectrum. Star symbols show empirically determined acoustic fluxes by Deubner[39].

shock heating has sufficient power to balance the observed cooling rates. The same very likely is the case for the heating of chromospheric magnetic flux tubes, where the shock heating is by longitudinal tube waves. Note as discussed in the review[30], this is different in the transition layer where in addition other types of heating, like microflare heating become important.

4. Weak shock heating and the generation of acoustic waves

Small-amplitude acoustic shock waves behave essentially like acoustic waves, except that they dissipate at the shock front (see below). In particular, the amplitude relations are identical. Consider linear small-amplitude sawtooth waves with pressure and velocity variations $p = p_0 + p_m - 2p_m t/P$, $v = v_m - 2v_m t/P$, where P is the wave period, t the time and subscript m indicates maximum amplitudes, the wave energy flux (erg cm^{-2} s^{-1}) is given by:

$$F_{\mathrm{M}} = \frac{1}{P}\int_0^P (p - p_0) v \, dt = \frac{1}{3} p_m v_m \approx \frac{1}{12}\gamma p_0 c_S \eta^2, \quad (11)$$

where p_0 is the unperturbed pressure, c_S the sound speed, γ the ratio of specific heats and where for weak shocks one has for the total pressure, velocity, temperature and density jumps $2p_m \approx \gamma p_0 \eta$, $2v_m \approx c_S \eta$, $2T_m \approx (\gamma - 1)T_0 \eta$, $2\rho_m \approx \rho_0 \eta$. Here the shock strength is defined as $\eta = (\rho_2 - \rho_1)/\rho_1$, where ρ_1, ρ_2 are the densities in front and behind the shock[31]. By expanding the entropy jump ΔS per unit mass at the shock front, the shock dissipation rate (erg cm^{-3} s^{-1}) of the wave can be written

$$\Phi_{\mathrm{M}} = \frac{\rho T \Delta S}{P} = \frac{\rho_0 c_S^2}{\gamma(\gamma-1)P} \ln\left(\frac{p_2}{p_1}\left(\frac{\rho_2}{\rho_1}\right)^{-\gamma}\right) \approx \frac{1}{12}\frac{\gamma(\gamma+1)}{P} p_0 \eta^3. \quad (12)$$

The approximate equality is only valid for weak shocks where the entropy jump is small. Let us assume a gravitational atmosphere and in analogy to ray optics that the quantity $F_{\mathrm{M}} c_S^2$ is conserved. Differentiating eq. (11) with respect to height z and using (12) gives an equation for the shock strength

$$\frac{d\eta}{dz} = \frac{\eta}{2}\left(\frac{\gamma g}{c_S^2} - \frac{3}{2c_S^2}\frac{dc_S^2}{dz} - \frac{(\gamma+1)\eta}{c_S P}\right), \quad (13)$$

where g is the gravitational acceleration. The refractive term involving dc_S^2/dz is small in the chromosphere and can be neglected. For an isothermal, nonionizing, gravitational atmosphere eq. (13) can be solved for various initial shock strength's η_0 and shows that irrespective of the η_0 the shocks eventually reach a *limiting shock strength* η^{lim} given by

$$\eta^{\mathrm{lim}} = \frac{\gamma g P}{(\gamma+1)c_S}. \quad (14)$$

From eq. (11) one obtains a limiting wave energy flux

$$F_M^{\mathrm{lim}} = \frac{1}{12}\frac{\gamma^3 g^2 P^2}{(\gamma+1)^2 c_S} p_0. \quad (15)$$

Eq. (13) has the property that for small shock strengths one initially has an exponential growth due to flux conservation which results from the first term on the RHS of the equation. This growth of the sawtooth wave is similar to that for acoustic waves in a gravitational atmosphere assuming flux conservation, $\rho_0 v^2 \sim \rho_0 c_S^2 \eta^2 = \mathrm{const}$. The increase in shock strength is eventually balanced by the increasing shock dissipation described by the last term of eq. (13). Limiting strength is reached when η becomes constant and the flux proportional to the gas pressure p_0.

Figure 2 shows limiting-strength acoustic-heating fluxes $F_{\mathrm{M}}^{\mathrm{lim}}$ for wave periods $P = P_A/5$ and $P = P_A/10$, where $P_A = 4\pi c_S/(\gamma g)$ is the acoustic cut-off period. It is seen that the fluxes $\log F_{\mathrm{M}}^{\mathrm{lim}}$ rise linearly with the logarithm of the mass column density m, since $m = p_0/g$ and from eq. (15) $F^{\mathrm{lim}} \sim p_0$. The figure therefore shows that acoustic shock waves are able to explain the observed height dependence of the chromospheric emission. As will be shown below, acoustic wave generation calculations for the solar convection zone by Musielak *et al.*[32] also provide the correct wave period for Figure 2. As shown below one finds that $P = P_A/5$ is roughly the period of the maximum of the acoustic-wave spectrum generated in the convection zone. Using this value one has from the above equations

$$\eta^{\mathrm{lim}} = \frac{1}{5}\frac{4\pi}{\gamma+1} = 0.94, \quad (16)$$

$$F_{\mathrm{M}}^{\mathrm{lim}} = \frac{4\pi^2}{75}\frac{\gamma}{(\gamma+1)^2} c_S p_0 \approx 0.123 c_S p_0 \approx 10^5 p_0 \approx 2.4\times10^9 \, m, \quad (17)$$

and a heating rate per gram

$$\frac{1}{\rho}\frac{dF_{\mathrm{M}}}{dz}\bigg|_{\mathrm{lim}} = \frac{dF_{\mathrm{M}}}{dm} = \frac{\Phi_{\mathrm{M}}}{\rho} = \frac{4\pi^2}{75}\frac{\gamma}{(\gamma+1)^2} c_S g \approx 2.4 \times 10^9 \ \mathrm{erg\ g^{-1}\ s^{-1}}. \quad (18)$$

The computation of the generation of acoustic energy in stellar convection zones dates to the theory of quadrupole sound generation from turbulence developed by Lighthill[33,34] and Proudman[35]. Considering a

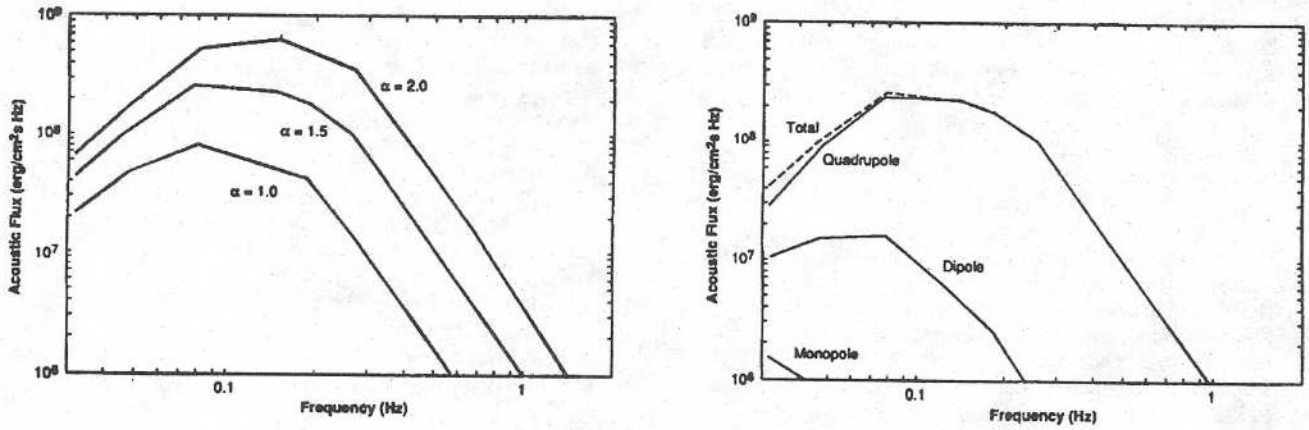

Figure 3. Acoustic wave spectra for different values of the mixing-length parameter α (*left panel*), different contributions to the acoustic spectrum (*right panel*), computed with the Lighthill–Stein theory, after Musielak *et al.*[32].

Kolmogorov turbulence spectrum, Lighthill has derived an expression

$$F_M = \int 38 \frac{\rho_0 u^8}{c_S^5 H} dz, \tag{19}$$

called *Lighthill formula*, where z is height, H is the scale height, ρ_0 the density, c_S the sound speed and u the turbulent velocity. This famous u^8-formula was found to be in excellent agreement with measurements in terrestrial applications. Lighthill's theory was further extended by Stein[36,37] to allow for the computation of the acoustic frequency spectrum and was recently revisited[32]. To compute the acoustic flux using the Lighthill–Stein theory, one must first calculate a convection zone model where one uses the mixing-length theory, which depends on a free parameter, the mixing-length parameter α. Musielak *et al.*[32] on the basis of a description of the turbulence with an extended Kolmogorov spectrum and a modified Gaussian frequency factor, found total acoustic fluxes $F_M = 1.3 \times 10^7$ erg cm^{-2} s^{-1} for $\alpha = 1.0$ and 1.7×10^8 erg cm^{-2} s^{-1} for $\alpha = 2.0$.

Figure 3 shows the acoustic spectra obtained by these authors and demonstrates that quadrupole generation (also used in the Lighthill formula) is the most important contribution to the acoustic-wave flux. Since the frequencies in Figure 3 are circular frequencies, the spectra have a maximum at periods $P = 79$, 58 and 41 s for $\alpha = 1.0$, 1.5, 2.0, respectively. Recent numerical convection zone calculations show that α, the ratio of the mixing-length L to the scale height H, typically varies only in a narrow range of $\alpha \approx 2.0$–2.16 (ref. 38). Taking a temperature $T = T_{\text{eff}} = 5770$ K, the acoustic cut-off period is found to be 216 s such that $P = P_A/5 = 43$ s is a good estimate for the maximum of the generated solar acoustic wave spectrum. Note that Figure 2 shows also empirical acoustic fluxes by Deubner[39] which are in rough agreement with the empirical losses.

5. Conclusions

Waves are responsible for the characteristic features of the chromosphere: the permanent outward temperature rise, which is due to acoustic waves that dissipate in shocks, the 3-min oscillations of the nonmagnetic chromosphere, whose period matches the cutoff period of acoustic waves, and the 7-min oscillations, whose period matches the cutoff period of transverse flux tube waves for a pressure ratio of $\beta \approx 0.25$.

The empirical radiative emission rate of the chromosphere can be understood on the basis of the dissipation rate of weak-shock theory, and the appearance of the cutoff periods in the chromospheric oscillations can be understood as due to impulsive or stochastic wave excitation, which causes the atmosphere behind the head of a wave to oscillate at the cutoff period.

1. Lites, B. W., Rutten, R. J. and Kalkofen, W., *Astrophys. J.*, 1993, **414**, 345.
2. von Uexküll, M. and Kneer, F., *Astron. Astrophys.*, 1995, **294**, 252.
3. Grossmann-Doerth, U., Kneer, F. and von Uexküll, M., *Solar Phys.*, 1974, **37**, 85.
4. Carlsson, M., Judge, P. G. and Wilhelm, K., *Astrophys. J.*, 1997, **486**, L63.
5. Curdt, W. and Heinzel, P., *Astrophys. J.*, 1998, **503**, L95.
6. Vernazza, J. E., Avrett, E. H. and Loeser, R., *Astrophys. J. (Supplement)*, 1981, **45**, 635.
7. Carlsson, M. and Stein, R. F., in *Chromospheric Dynamics*, Proceedings of the Mini-Workshop, Institute for Theoretical Astrophysics, Oslo, 1994.
8. Carlsson, M. and Stein, R. F., in *IAU Symposium 185* (eds Deubner, F.-L., Christensen-Dalsgaard, J. and Kurtz, D.), Kluwer, Dordrecht, 1998, 435.
9. Spruit, H. C., in *The Sun as a Star* (ed. Jordan, S.), NASA Monograph Series on Nonthermal Phenomena in Stellar Atmospheres, 1981, p. 385.
10. Damé, L., Thèse, Université de Paris, VII, 1983.
11. Damé, L., in *Small-Scale Dynamical Processes in Quiet Stellar Chromospheres* (ed. Keil S. L.), NSO/SPO, Sunspot, NM, 1984, p. 54.

12. Lou, Y.-Q., *MNRAS*, 1995, **276**, 769.
13. Deubner, F.-L. and Fleck, B., *Astron. Astrophys.*, 1990, **228**, 506.
14. Kalkofen, W., *Astrophys. J.*, 1997, **486**, L145.
15. Choudhuri, A. R., Auffret, H. and Priest, E. R., *Solar Phys.*, 1993, **143**, 49.
16. Kalkofen, W., Rossi, P., Bodo, G. and Massaglia, S., *Astron. Astrophys.*, 1994, **284**, 976.
17. Zhugzhda, Y. D., Bromm, V. and Ulmschneider, P., *Astron. Astrophys.*, 1995, **300**, 302.
18. Ulmschneider, P., Zähringer, K. and Musielak, Z. E., *Astron. Astrophys.*, 1991, **241**, 625.
19. Hasan, S. S. and Kalkofen, W., *Astrophys. J.*, 1999, (in press).
20. Rae, I. C. and Roberts, B., *Astrophys. J.*, 1982, **256**, 761.
21. Lamb, H., *Proc. Lond. Math. Soc.*, 1909, **7**, 122.
22. Spruit, H. C. and Roberts, B., *Nature*, 1983, **304**, 401.
23. Goode, P. R., Strous, L. H., Rimmele, T. R. and Stebbins, R. T., *Astrophys. J.*, 1998, **495**, L27.
24. Sutmann, G. and Ulmschneider, P. *Astron. Astrophys.*, 1995, **294**, 232.
25. Liu, S.-Y., *Astrophys. J.*, 1974, **189**, 359.
26. Muller, R. and Roudier, Th., Vigneau, J. and Auffret, H., *Astron. Astrophys.*, 1994, **283**, 232.
27. Theurer, J., Ulmschneider, P. and Kalkofen, W. *Astron. Astrophys.*, 1997, **324**, 717.
28. Kalkofen, W., Ulmschneider, P. and Avrett, E. H., *Astrophys. J. (Lett.)*, 1999, **521**, (in press).
29. Anderson and Athay, *Astrophys. J.*, 1989, **346**, 1010.
30. Narain, U. and Ulmschneider, P., *Space Sci. Rev.*, 1996, **75**, 453.
31. Ulmschneider, P., *Solar Phys.*, 1970, **12**, 403.
32. Musielak, Z. E., Rosner, R., Stein, R. F. and Ulmschneider, P., *Astrophys. J.*, 1994, **423**, 474.
33. Lighthill, M. J., *Proc. R. Soc. London*, 1952, **A211**, 564.
34. Lighthill, M. J., *Proc. R. Soc. London*, 1954, **A222**, 1.
35. Proudmann, I., *Proc. R. Soc. London*, 1952, **A214**, 119.
36. Stein, R. F., *Solar Phys.*, 1967, **2**, 385.
37. Stein, R. F., *Astrophys. J.*, 1968, **154**, 297.
38. Trampedach, R., Christensen-Dalsgaard, J., Nordlund, A., Stein, R. F., in *Solar Convection and Oscillations and their Relationship* (eds Pijpers, F. P., Christensen-Dalsgaard, J., Rosenthal, C. S.), 1997, p. 73.
39. Deubner, F.-L., in *Pulsation and Mass Loss in Stars* (eds Stalio, R., Willson, L. A.), Kluwer, 1988, p. 163.

ACKNOWLEDGEMENTS. W.K. thanks his colleagues at the Institut für Theoretische Astrophysik for their hospitality and the University of Heidelberg for a Mercator guest professorship funded by the DFG. Partial support by NASA is acknowledged.

CURRENT SCIENCE

SUBMISSION IN ELECTRONIC FORM

Authors who have been informed of acceptance of their manuscripts may send the final version in electronic form on floppy diskette (3.5" preferred; IBM PC format only, *not* Mackintosh). The text of the manuscript only should be supplied as a plain ASCII file with no formatting other than line and paragraph breaks. (WordStar 5.5 or 7.0 and Microsoft Word for Windows 6.0 are acceptable, but ASCII is preferred.) A hard copy of the text, with all typesetting information (italics, bold, mathematical type, superscripts, subscripts, etc.) must accompany the electronic copy. Tables and figures must be supplied only as hard copy. The diskette must be labeled clearly with the following: manuscript number, file name, file information (ASCII or WordStar, version number, etc.).

Text may also be transmitted as ASCII only by e-mail to currsci@ias.ernet.in.

We expect that electronic submission will result in quicker processing for publication.